Fabrication and optical properties of Ce-doped ZnO nanorods

Jihui Lang, Qiang Han, Jinghai Yang, Changsheng Li, Xue Li et al.

Additional information on J. Appl. Phys.

Fabrication and optical properties of Ce-doped ZnO nanorods

Jihui Lang,[1,2] Qiang Han,[1,2] Jinghai Yang,[1,a)] Changsheng Li,[2] Xue Li,[1] Lili Yang,[1] Yongjun Zhang,[1] Ming Gao,[1] Dandan Wang,[1,3] and Jian Cao[1,3]

[1]*Institute of Condensed State Physics, Jilin Normal University, Siping 136000, People's Republic of China*
[2]*School of Material Science and Engineering, Jiangsu University, Zhenjiang 212013, People's Republic of China*
[3]*Key Laboratory of Excited State Physics, Changchun Institute of Optics, Fine Mechanics and Physics, Chinese Academy of Sciences, 3888 Eastern Nan-Hu Road, Changchun 130033, People's Republic of China*

Ce-doped ZnO nanorods were prepared under mild hydrothermal condition. The microstructures, morphologies and optical properties of as-synthesized nanorods were investigated by x-ray diffraction (XRD), transmission electron microscope (TEM), x-ray photoelectron spectroscopy (XPS), photoluminescence spectroscopy (PL), and Raman spectroscopy. XRD and XPS results demonstrated that Ce ions were successfully incorporated into the lattice position of Zn ions in ZnO. TEM images illustrated that the average diameter of Ce-doped ZnO nanorods was 8 nm. PL measurements revealed that both the undoped and Ce-doped ZnO nanorods had an UV emission and a defect emission and the Ce ions doping induced a redshift in the UV emission and a small enhancement in the defect emission. The slight shift in A_{1L} and E_{1L} in Raman spectra increased with the Ce ions doping also indicated that the Ce doping changed the free carrier concentration in the ZnO nanorods. © *2010 American Institute of Physics*. [doi:10.1063/1.3318613]

I. INTRODUCTION

Recently, rare-earth (RE) ion doped semiconductors have become the focus of numerous investigations because of their unique optical properties and promising applications in optoelectronic devices.[1–5] Since ZnO has a wide band-gap energy of 3.37 eV at room temperature, its nanocrystals are the suitable host materials for the doping elements such as RE and transition metal ions which are optically and magnetically active.[6–10] For the RE-doped ZnO nanocrystals, they are expected to be potential candidate materials for flat panel displays due to their possibility for efficiently emission in the visible range. Furthermore, ZnO is one of the environmental friendly materials, the RE-doped ZnO nanocrystals can also be used as florescence labels for biological imaging. Until now, different synthesis routes have been developed for the preparation of RE-doped ZnO nanostructures such as pulsed laser deposition, thermal evaporation, magnetron sputter deposition, pyrolysis, wet chemical etching, and chemical-combustion process.[11–19] However, the reports about the growth of small-scale RE-doped ZnO nanorods under low temperature and, in particular, the effects of the dopant on the structures and optical properties are limited.[20–22]

In this paper, we explore a mild hydrothermal route to prepare the Ce-doped ZnO nanorods and successfully control the crystallization of samples. Moreover, the optical properties of the as-synthesized Ce-doped ZnO nanorods are investigated in detail.

II. EXPERIMENTAL

In typical experiment, $Zn(Ac)_2 \cdot 2H_2O$ (99.9% purity) and $Ce(NO_3)_3 \cdot 6H_2O$ (99.9% purity) were dissolved in ethanol solution. The appropriate amounts of NaOH (99.9% purity) solution in ethanol was added to the above solution. The mixture was stirred for 10 min and then transferred to a telfon-lined stainless steel autoclave heated at 150 °C for 24 h. Subsequently, the system was allowed to cool to room temperature. The final product was collected, washed with deionized water and ethanol for several times, separated by a centrifuge, and then dried in an oven under 60 °C.

XRD (MAC Science, MXP18, Japan), TEM (JEM-2100HR, Japan), XPS (VG ESCALAB Mark II), PL (He–Cd Laser, 325 nm) and Raman (Invia-UV, U.K.) were used to characterize the crystal structures, morphologies, chemical composition, and optical properties of ZnO nanorods.

III. RESULTS AND DISCUSSION

Figure 1 shows the XRD patterns of the as-synthesized samples. All the diffraction peaks can be indexed to a hexagonal wurtzite ZnO structure and no peaks are detected from any other impurities. The sharp diffraction peaks in the XRD patterns indicate that the ZnO prepared with the present method are highly crystallized. The diffraction peaks of Ce-doped ZnO shift slightly toward the lower angle, indicating that the lattice parameters are a little larger than those of undoped ZnO. We also calculate the lattice parameters from XRD patterns. The lattice parameters (a=3.245684, c=5.201863) of the Ce-doped ZnO increase compared with the undoped one (a=3.243466 and c=5.198402), which indicates that Ce ions have been incorporated into the ZnO

---

a)Author to whom correspondence should be addressed. Tel.: +86 434 3294566. FAX: +86 434 3294566. Electronic mail: jhyang1@jlnu.edu.cn.
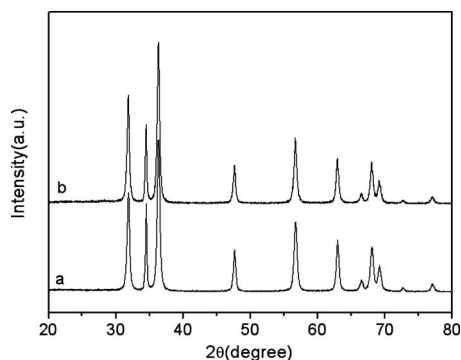
     107, 074302-1

FIG. 1. XRD patterns of ZnO nanorods doped with Ce ions: (a) undoped and (b) doped with 1% Ce in molarity.

lattice and substituted the Zn ion sites because the ionic radius of Ce^{4+} (0.92 Å) is much bigger than that of Zn^{2+} (0.74 Å).

Figure 2 shows the TEM images of the undoped and Ce-doped ZnO. The images clearly reveal that the samples are composed of uniform nanorods. From the Figs. 2(b) and 2(c), it can be seen that the average diameter of the Ce-doped ZnO nanorods is about 8 nm, which is much smaller than that of the previous techniques we used such as chemical solution deposition method, sol-gel method, etc.[23–25] Moreover, the average diameter of the Ce-doped ZnO nanorods is a little bigger than the undoped one and the image contrasts of undoped and Ce-doped nanorods are different, indicating that Ce ions have been incorporated into the nanorods.

Figure 3(a) shows a typical XPS spectra of the as-synthesized Ce-doped ZnO nanorods. The high resolution scans of Ce $3d$ and O $1s$ are shown in the Figs. 3(b) and 3(c). We would like to mention that, in all the XPS spectra, the binding energies have been calibrated by taking the carbon C $1s$ peak (285.0 eV) as reference. The peaks located at 1022 and 1045 eV are associated to Zn $2p_{3/2}$ and Zn $2p_{1/2}$, respectively. In the O $1s$ region, there are two distinct components to the observed peak shape: an intense low-energy component at 530 eV and a high energy component at 531.3
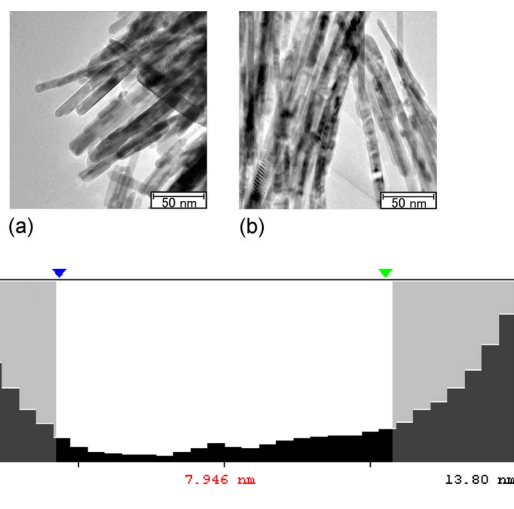

FIG. 2. (Color online) TEM images of ZnO nanorods doped with Ce ions: (a) undoped, (b) doped with 1% Ce in molarity, and (c) the image of diameter for a nanorod [sample (b)].
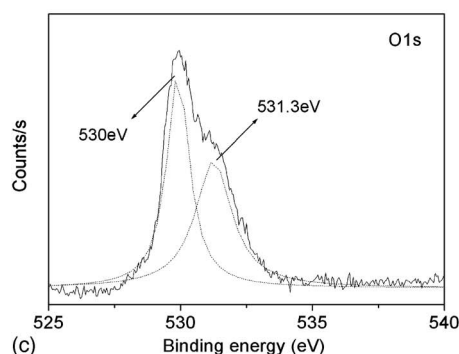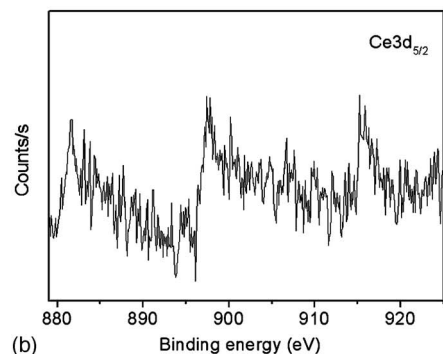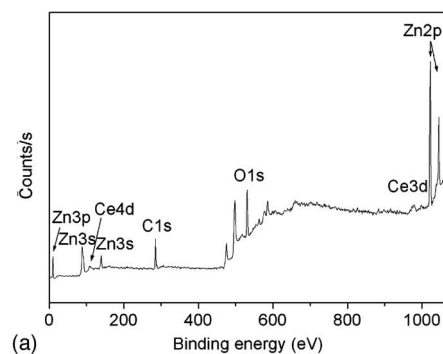

FIG. 3. XPS spectrum of ZnO nanorods doped with 1% Ce ions in molarity.

eV. The high resolution scans also show that the binding energy of Ce $3d_{5/2}$ is located at 881.9, 897.4, and 915.2 eV, which clearly indicates that the Ce ions has a +4 oxidation valance state.[26] It is well known that Ce ions have two different oxidation states of Ce^{4+} and Ce^{3+}. But the Ce^{4+} oxidation state is very stable compared with the Ce^{3+} oxidation state in the presence of air. The binding energy of Ce $3d_{5/2}$ for the Ce-doped ZnO nanorods exhibits slight blueshift compared with the standard XPS energy peak locations of Ce $3d_{5/2}$ in CeO_2.[26] The slight shift indicates that the Ce–O bond length in ZnO has changed due to Ce^{4+} ions incorporating into the ZnO lattices, which is similar to ZnO: Tb thin films.[13] It can be explained that the Ce–O bond length should be decreased when Ce ions have been incorporated into the ZnO lattice and substituted the Zn ion sites because the ionic radius of Ce^{4+} is much bigger than that of Zn^{2+}. Such shrink of the Ce–O bond length increases the interaction between ions and causes the slight blueshift in the Fig. 3(b). In addition, no signals of other impurities are detected from the Fig. 3, implying the synthesis of Ce^{4+}-doped ZnO nanorods.

Figure 4 shows the photoluminescence (PL) spectra of the undoped and Ce-doped ZnO nanorods measured at room
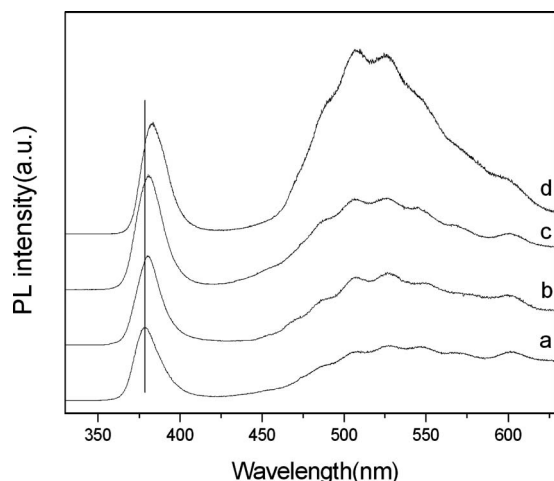
FIG. 4. Room temperature PL spectra of ZnO nanorods doped with Ce ions: (a) undoped, (b) doped with 0.5% Ce in molarity, (c) doped with 1% Ce in molarity, and (d) doped with 2% Ce in molarity.

FIG. 5. Raman spectra of ZnO nanorods doped with Ce ions: (a) undoped and (b) doped with 1% Ce in molarity.

temperature. The PL is excited by a He–Cd laser at a wavelength of 325 nm. As seen in Fig. 4, the positions of UV emission from Ce-doped ZnO nanorods with various doping concentration (0%, 0.5%, 1%, and 2% in molarity) are located at 379.134, 379.839, 380.543, and 383.361 nm, respectively. The UV emission originates from the recombination of the free excitons of ZnO.[27–29] When Ce ions as the donors are incorporated into ZnO, the bandgap structure of ZnO nanorods will be modulated substantially and new emission centers are formed, which leads to the slight redshift in the UV emission.[30,31] Briefly, the substitutional Ce^{4+} ions form the Ce electron localized states and introduce electron states (i.e., impurity band) into the band gap of ZnO. These electron states locate closer to the lower edge of the conduction band to form the new lowest unoccupied molecular orbital, which results in the band gap reduction and eventually makes the redshift in UV emission in this case.

In addition, as shown in Fig. 4, the broad green emission also exists in the PL spectra, which originates from the electron-hole recombination at the defect sites due to electron transition from the shallow donor level of the intrinsic defect centers, such as interstitial zinc and oxygen vacancy to the valence or conduction band.[13,32,33] In comparison with the PL spectra, it can be observed that Ce doping into the ZnO nanorods could effectively quench the UV emission and enhance the green emission. The enhanced intensity of the green emission confirms that the increased density of defects,[32,34,35] which could be attributed to the oxygen vacancy introduced by the existence of Ce impurities in ZnO nanorods.

Raman scattering is very sensitive to the microstructure of nanosized materials. It is a nondestructive characterization method for studying vibrational properties of ZnO nanostructures. Raman scattering is used here to clarify the quality and structure of ZnO nanorods.

Wurtzite-type ZnO belongs to the space group C_{6v}^4 with two formula units in the primitive cell. The optical phonons at Γ point of the Brillouin zone belong to the following irreducible representation: $\Gamma_{opt} = 1A_1 + 2B_1 + 2E_1 + 2E_2$.[36] For op-
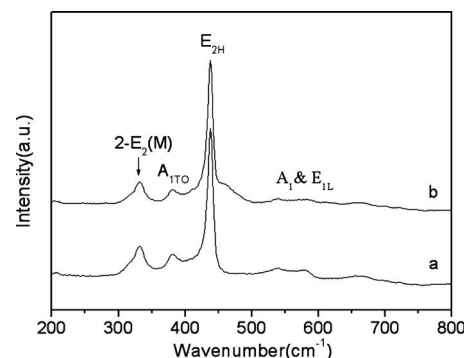
tical modes, B_1 modes are Raman silent modes. For the long-range electrostatic forces, both A_1 and E_1 modes are polar and are split into transverse optical and longitudinal optical (LO) phonons. A nonpolar phonon mode with symmetry E_2 has two frequencies, E_{2H} is associated with oxygen atoms and E_{2L} is associated with Zn sublattice. Among the optical modes, A_1, E_1, and E_2 are Raman active.

Figure 5 shows the Raman spectra of the undoped and Ce-doped ZnO nanorods excited by the 514 nm line of an argon laser. From the Fig. 5(b), the peaks located at 331.5, 379.8, 438.1, and 582.3 cm^{-1} can be observed. The peaks located at 331.5, 379.8, and 438.1 cm^{-1} can be assigned to second-order Raman spectrum $2E_2(M)$, A_{1T}, and E_{2H}, respectively. The strongest peak centered at about 438.1 cm^{-1} is characteristic mode (E_{2H}) for the hexagonal phase of ZnO.[25,37] The E_{2H} mode can be observed in the Raman spectra from all samples, which indicates the good crystallization of the nanorods and further testifies the results from XRD patterns. In addition, a broad peak located at 582.3 cm^{-1} can be also observed. Usually, the peak located at 574 cm^{-1} in bulk ZnO corresponded to A_{1L} phonon can be observed only in the configuration when the c-axis of wurtzite ZnO is parallel to the sample face. When the c-axis is perpendicular to the sample face, the E_{1L} (591 cm^{-1}) phonon is observed, instead.[38] According to the theory of polar optical phonons in wurtzite nanocrystals,[39,40] the frequency of 1LO phonon mode in ZnO should be between 574 and 591 cm^{-1}. So the peak around 582.3 cm^{-1} is contributed to the superimposition of A_{1L} and E_{1L}.

In addition, the position of the peak (A_{1L} and E_{1L}) is about 582.3 cm^{-1} for the Ce-doped ZnO nanorods, and that of the undoped one is about 578.9 cm^{-1}. It can be seen that the position of A_{1L} and E_{1L} peak shift to higher wavenumber compared with the undoped ZnO, which may be due to the point defects such as oxygen vacancies or zinc interstitials.[41,42] Moreover, the slight shift increases with the Ce doping also indicates that the Ce doping can change the free carrier concentration in the ZnO nanorods.

IV. CONCLUSION

In conclusion, Ce-doped ZnO nanorods are synthesized by the hydrothermal method. The results demonstrate that the Ce dopant has a strong effect on the structure and PL characteristics of ZnO nanorods, which could be caused by

the increasing lattice defects due to the Ce doping. The diameter of the Ce-doped ZnO nanorods is about 8 nm, which is much smaller than that of the previous techniques we used such as chemical solution deposition method, sol-gel method, etc. PL and Raman measurements show that the doped sample retains its high quality and good PL behaviors. The redshift in the UV emission is due to the band gap narrowing caused by the downshift in the conduction band edge after merging with the cerium related impurity band formed below the conduction band. The synthesis of the Ce-doped nanorods could present a new potential application in photoelectric nanodevices. Also the growth technique can be applied to fabricate other hierarchical doping semiconductors with small diameter.

ACKNOWLEDGMENTS

[1] Z. K. Tang, G. K. L. Wang, and P. Yu, Appl. Phys. Lett. **72**, 3270 (1998).
[2] Z. Zhou, T. Komori, T. Ayukawa, H. Yukawa, M. Morinaga, A. Koizumi, and Y. Takeda, Appl. Phys. Lett. **87**, 091109 (2005).
[3] X. D. Wang, J. H. Song, J. Liu, and Z. L. Wang, Science **316**, 102 (2007).
[4] L. Armelao, F. Heigl, A. Jurgensen, R. I. R. Blyth, T. Regier, X.-T. Zhou, and T. K. Sham, J. Phys. Chem. C **111**, 10194 (2007).
[5] J. Song, X. Wang, J. Liu, H. Liu, Y. Li, and Z. Wang, Nano Lett. **8**, 203 (2008).
[6] H. Liu, J. Yang, Y. Zhang, Y. Wang, and M. Wei, Mater. Chem. Phys. **112**, 1021 (2008).
[7] K. R. Kittilstved, J. Zhao, W. K. Liu, J. D. Bryan, D. A. Schwartz, and D. R. Gamelin, Appl. Phys. Lett. **89**, 062510 (2006).
[8] A. Ishizumi and Y. Kanemitsu, Appl. Phys. Lett. **86**, 253106 (2005).
[9] Y. Liu, T. Tan, B. Wang, X. Song, E. Li, H. Wang, and H. Yan, J. Appl. Phys. **103**, 056104 (2008).
[10] E.-J. Kan, L.-F. Yuan, and J. Yang, J. Appl. Phys. **102**, 033915 (2007).
[11] J.-R. Duclère, B. Doggett, M. O. Henry, E. McGlynn, R. T. Rajendra Kumar, J.-P. Mosnier, A. Perrin, and M. Guilloux-Viry, J. Appl. Phys. **101**, 013509 (2007).
[12] R. Pérez-Casero, A. Gutiérrez-Llorente, O. Pons-Y-Moll, W. Seiler, R. M. Defourneau, D. Defourneau, E. Millon, J. Perrière, P. Goldner, and B. Viana, J. Appl. Phys. **97**, 054905 (2005).
[13] X. M. Teng, H. T. Fan, S. S. Pan, C. Ye, and G. H. Li, J. Appl. Phys. **100**, 053507 (2006).
[14] J. S. John, J. L. Coffer, Y. Chen, and R. F. Pinizzotto, Appl. Phys. Lett. **77**, 1635 (2000).
[15] J. L. Bubendorff, J. Ebothe, A. El Hichou, R. Dounia, and M. Addou, J. Appl. Phys. **100**, 014505 (2006).
[16] M. Alaoui Lamrani, M. Addou, Z. Soofiani, B. Sahraoui, J. Ebothé, A. El Hichou, N. Fellahi, J. C. Bernède, and R. Dounia, Opt. Commun. **277**, 196 (2007).
[17] Z. Sofiani, S. Bouchta, and M. Addou, J. Appl. Phys. **101**, 063104 (2007).
[18] N. Mais, J. P. Reithmaier, A. Forchel, M. Kohls, L. Spanhel, and G. Müller, Appl. Phys. Lett. **75**, 2005 (1999).
[19] Y. Liu, Q. Yang, and C. Xu, J. Appl. Phys. **104**, 064701 (2008).
[20] Juan Wang, M. J. Zhou, S. K. Hark, Quan Li, D. Tang, M. W. Chu, and C. H. Chen, Appl. Phys. Lett. **89**, 221917 (2006).
[21] S. Z. Li, C. L. Gan, H. Cai, C. L. Yuan, J. Guo, P. S. Lee, and J. Ma, Appl. Phys. Lett. **90**, 263106 (2007).
[22] L. Yang, Y. Tang, A. Hu, X. Chen, K. Liang, and L. Zhang, Physica B **403**, 2230 (2008).
[23] L. L. Yang, Q. X. Zhao, M. Willander, J. H. Yang, and I. Ivanov, J. Appl. Phys. **105**, 053503 (2009).
[24] J. Yang, M. Gao, L. Yang, Y. Zhang, J. Lang, D. Wang, Y. Wang, H. Liu, and H. Fan, Appl. Surf. Sci. **255**, 2646 (2008).
[25] J. Yang, J. Lang, C. Li, L. Yang, Q. Han, Y. Zhang, D. Wang, M. Gao, and X. Liu, Appl. Surf. Sci. **255**, 2500 (2008).
[26] C. D. Wagner, W. M. Riggs, L. E. Davis, J. F. Moulder, and G. E. Muilenberg, *Handbook of X-Ray Photoelectron Spectroscopy*, (Perkin-Elmer Corporation, Physical Electronics Division, Eden Prairie, Minn., 1979).
[27] D. Weissenberger, M. Dürrschnabel, D. Gerthsen, F. Pérez-Willard, A. Reiser, G. M. Prinz, M. Feneberg, K. Thonke, and R. Sauer, Appl. Phys. Lett. **91**, 132110 (2007).
[28] W. I. Park, Y. H. Jun, S. W. Jung, and G.-C. Yi, Appl. Phys. Lett. **82**, 964 (2003).
[29] D. C. Reynolds, D. C. Look, and B. Jogai, Phys. Rev. B **57**, 12151 (1998).
[30] A. Majid and A. Ali, J. Phys. D **42**, 045412 (2009).
[31] W. Li, Y. Wang, H. Lin, S. Ismat Shah, C. P. Huang, D. J. Doren, S. A. Rykov, J. G. Chen, and M. A. Barteau, Appl. Phys. Lett. **83**, 4143 (2003).
[32] K. Vanheusden, C. H. Seager, W. L. Warren, D. R. Tallant, and J. A. Voiget, Appl. Phys. Lett. **68**, 403 (1996).
[33] G.-R. Li, X.-H. Lu, W.-X. Zhao, C.-Y. Su, and Y.-X. Tong, Cryst. Growth Des. **8**, 1276 (2008).
[34] S. Y. Bae, H. C. Choi, C. W. Na, and J. Park, Appl. Phys. Lett. **86**, 033102 (2005).
[35] W. S. Shi, O. Agyeman, and C. N. Xu, J. Appl. Phys. **91**, 5640 (2002).
[36] G. Xiong, U. Pal, and J. Garcia Serrano, J. Appl. Phys. **101**, 024317 (2007).
[37] L. Yang, J. Yang, X. Liu, Y. Zhang, Y. Wang, H. Fan, D. Wang, and J. Lang, J. Alloys Compd. **463**, 92 (2008).
[38] N. Ashkenov, B. N. Mbenkum, C. Bundesmann, V. Riede, M. Lorenz, D. Spemann, E. M. Kaidashev, A. Kasic, M. Schubert, and M. Grundmann, J. Appl. Phys. **93**, 126 (2003).
[39] V. A. Fonoberov and A. A. Balandin, Phys. Rev. B **70**, 233205 (2004).
[40] V. A. Fonoberov and A. A. Balandin, Phys. Status Solidi C **1**, 2650 (2004).
[41] Y. Huang, M. Liu, Z. Li, Y. Zeng, and S. Liu., Mater. Sci. Eng., B **97**, 111 (2003).
[42] W. Da, S. Wu, K. Liu, W. Chen, and S. Pan, Chinese Journal of Light Scattering **18**, 43 (2006).